Computational Drug Design of Cyclotide-Based Inhibitors Targeting Crimean–Congo Hemorrhagic Fever Virus: An Integrative Molecular Docking and Dynamics Approach

Mansoor Alsahag, Msc, PhD*

ABSTRACT

Crimean–Congo haemorrhagic fever (CCHF) is a highly pathogenic zoonotic disease caused by a negative-sense single-stranded RNA virus of the *Nairoviridae* family and *Orthonairovirus* genus. The virus targets endothelial and immune cells, leading to immune evasion and vascular damage. This study employs computational modelling to evaluate cyclotides as potential antiviral agents targeting the glycoprotein of the CCHF viral envelope to mitigate its pathogenicity. The target protein (PDB ID: 8VVL) was retrieved from the Protein Data Bank, refined using PyMol, and its physicochemical properties were assessed via ProtParam. Cyclotides were obtained from the CyBase database, and 3D structures were modelled using Swiss Model for molecular docking analysis conducted via HDOCK. Toxicity and allergenicity predictions were performed, followed by molecular dynamics (MD) simulations for 100 ns using Desmond from Schrödinger LLC. The MMGBSA method was employed to estimate free binding energy. Physicochemical analysis indicated that the glycoprotein has a moderately hydrophilic nature (GRAVY: -0.113) with a theoretical isoelectric point of 8.06. Among the tested cyclotides, Kalata B7 demonstrated the highest docking score (-213.76 kcal/mol) and was identified as non-toxic and nonallergenic. MD simulations confirmed stable protein-ligand interactions, suggesting Kalata B7 as a promising therapeutic candidate. Further in vitro and in vivo studies are warranted to validate its potential for clinical application in combating CCHF.

Keywords: Crimean–Congo haemorrhagic fever (CCHF); Cyclotides; Molecular docking; Molecular dynamics simulations; Viral glycoprotein inhibition; Computational drug design

INTRODUCTION

The species, Crimean–Congo hemorrhagic fever (CCHF) causes severe hemorrhagic fever in humans. An RNA virus with negative-sense single stranded RNA genome is classified within the kingdom Orthornavirae, belongs to a family Nairoviridae and a member of genus Orthonairovirus. The order of Crimean–Congo hemorrhagic fever is Bunyavirales[1] .CCHF is primarily distributed through bites of infected Hyalomma tics to humans or in contact with tissue or blood, secretion or other body fluids of infected humans[2]. The highly pathogenic zoonotic virus has an ability to target endothelial cells, immune cells also lead to immune evasion and vascular damage. Farmers are at high risk of infection and those who are at slaughterhouses. The fatality rate is typically between 10% to 40% and high rate in some outbreaks observed as 80%[3]. Initially detected in the 1940s, in Crimea when local civilians and Soviet troops had severe hemorrhagic illnesses. During the 1960s, a similar virus was identified in Kisangani. Crimean–Congo hemorrhagic fever (CCHF) cases were observed in wide range including Russia, Africa, Middle East and Asia, also in Balkans[4]. There were 114 fatal cases out of 494 cases of Crimean–Congo hemorrhagic fever was reported in Africa between 1956 to 2020. Nine nations Nigeria, Kenya, Sierra Leone, South Sudan, Sudan and Tunisia, Senegal, Mali and Mozambique have reported the first case of CCHF[5]. Crimean–Congo hemorrhagic fever (CCHF) has a protective outer layer Gn known as envelope made up of Glycoproteins. Gn has a C-terminus section at the end which sticks to the cytoplasmic tail that helps to interact with the host cell[6]. The genetic material of the virus consists of segments which are S, M and L segments. The S segment protects the virus RNAs inside the cell. Its codes for the Nucleocapsid protein. M segments contain the instructions to make the viral Glycoprotein. While the L segment carries the Instructions to an enzyme the virus needs to replicate which is RNA dependent RNA polymerase[7].

After entering the human body, the virus starts its replication cycle and targets specific type of cells which are endothelial, epithelial cells and macrophages. It triggers both innate and adaptive immune responses[8]. The early stage of infection, which is known as pre-hemorrhage phase, the patient notices some symptoms such as fever, muscle aches, neck pain, dizziness and headache. While in acute infectious phase symptoms include nausea, diarrhea, vomiting with bleeding, abdominal pain and sore throat[9]. After a few days symptoms become more severe and lead to neurological disorders, a person may experience mood swings, confusion and restlessness[10]. As the infection proceeds the abdominal pain occurs on the upper right side and the liver becomes enlarged. The agitation becomes turn into sleepiness, fatigue and depression. As the illness moves into hemorrhage phase the symptoms become more transparent, including the bleeding at the injection sites, heavy nosebleeds, large bruises starting from the fourth day of infection and usually last for about 2 weeks[11]. Other signs include petechiae, a small rash under the mouth, skin or throat. This can turn into ecchymoses which is larger rashes, Tachycardia and Lymphadenopathy. After the 5th day, the liver shows some signs of hepatitis and in some cases, patients suffer from kidney failure, lungs problems and liver failure. The incubation period is typically from 2 to 3 days but can last as long as 9 days. While the incubation period within the infected blood or

* Faculty of Applied Medical Sciences
Al-Baha University, Al-Baha,
Kingdom of Saudi Arabia,
Email: maleshaq@bu.edu.sa

tissue usually lasts 5 to 6 days and maximum of 13 days[12].

There is no FDA and World Health Organization (WHO) approved drug available against this virus and no vaccine available commercially. Prevention involves avoiding contact with body fluids of infected animals or humans. To reduce the risk of tick-to-human transmission wear protective clothes and light-colored clothes for easy detection of ticks on clothes, use approved chemicals like repellent on skin and clothes, also avoid that type of areas where ticks are usually present[13]. To reduce the risk of animal-to-humans transmission wear protective gloves or clothes while handling animals during the procedure of slaughtering, culling and butchering. Routinely treat animals with pesticides two weeks before they enter slaughterhouses. To reduce the risk of human-to-human transmission avoid contact with CCHF infected people, wash hands regularly and wear protective gloves during take care of ill people[14].

One of the most comprehensive options for novel antiviral and antibacterial drugs is cyclotides, a class of cyclic peptides derived from plants. These peptides are incredibly stable due to their circular architectures and many disulfide connections[15]. Cyclotides have demonstrated remarkable effectiveness in combating bacterial, fungal, and viral infections. Their primary mode of action is to damage bacterial membranes, which leads to cell rupture and death. Cyclotides can be very important for creating novel medications to eradicate antibiotic-resistant microorganisms because of their remarkable ability to reverse superoxide anion, expression of antibacterial solid activity, and structural stiffness[16]. Future studies on the usage of cyclotides to treat Crimean–Congo hemorrhagic fever is valuable because of the pressing need to create new medications since drug resistance is becoming more prevalent.

METHODOLOGY

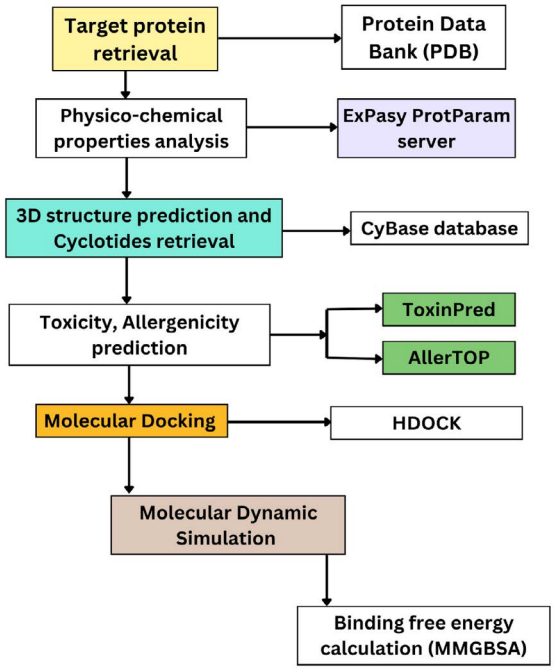

Figure 1. Methodology flowchart followed during the cyclotides based drug designing

Target protein retrieval and preparation: The target protein of Crimean–Congo hemorrhagic fever (CCHF) was retrieved from Protein Data Bank (http://www.rcsb.org) with the ID 8VVL , the extra water molecules and ligands were cleaned and visualized by PyMol[17]. Accurate modeling can be done with the PDB as it offers atomic-level information on protein structure. PDB format, which may be used to update the input for further computer research, was used to preserve the structure[18].

Physico-chemical properties: Physico-chemical properties of proteins were predicted through the ProtParam tool on the ExPasy server (https://web.expasy.org/protparam/),which express the physical, chemical and structural characteristics of proteins such as their hydrophobic and hydrophilic nature, shape, size, polarity charges and solubility etc. ExPasy ProtParam parameter involves molecular weight, extinction coefficient, Instability index, Theoretical isoelectric point, Aliphatic index, amino acid and atomic composition, Grand average of hydropathicity and provide the values of hydrophobicity and hydrophilicity of protein sequences[19]. And PSIPRED tool (http://bioinf.cs.ucl.ac.uk/psipred/) shows the charts cartoon which indicates the protein secondary structure components[20].

3D structure prediction and Cyclotides retrieval: Cyclotides were retrieved from the CyBase database in Fasta format (https://www.cybase.org.au/). CyBase is an integrated database and tool for cyclic peptides having unique stability and biological activity (often studies for potential application in drug design and therapeutic development[21]. 3D models were generated using the trRosseta (https://yanglab.qd.sdu.edu.cn/trRosetta/). trRosseta is an extension of Rosseta designed for rapid and accurate modeling and protein structure prediction[22].

Toxicity and Allergenicity prediction of selected Cyclotides: Toxicity and Allergenicity were predicted through the tools which are ToxinPred (https://webs.iiitd.edu.in/raghava/toxinpred/) specially designed for toxicity in peptides and proteins[23] and through AllerTOP (https://www.ddg-pharmfac.net/allertop_test/) predicting the allergenicity of peptides or protein to check whether this protein or peptide triggers an allergic reaction toward humans[24]. These tests are essential for determining the effectiveness and safety of cyclotides as medicinal substances. The protein-stability heatmap was determined using the Protein-Sol server (https://protein-sol.manchester.ac.uk/heatmap). Two heatmap graphs representing the data were produced: one for energy and one for charge[25].

Molecular Docking: Docking analysis were performed through HDOCK (http://hdock.phys.hust.edu.cn/). A web-based tool to analyze molecular interactions between protein DNA/RNA and protein-protein[26]. This platform combines both blind docking and template-based modeling. It generates a list of docked complexes based on their binding affinity or binding energy scores. The most advantageous binding interactions and their possible biological significance were determined by analyzing the data. The top-scoring 8vvl-kalata7B complex was docked, and PyMol[17] was used to identify the binding site. A comprehensive examination of the docking contact was interpreted using the PDBsum online tool[27].

Molecular Dynamic Simulations: MD simulations were run with Desmond from Schrödinger LLC for 100,000 picoseconds(100ns). Docking research yielded first 8vvl-kalata7B protein-ligand (cyclotide) combinations using static binding predictions[28]. Atomic motions in physiological contexts are predicted throughout time by MD simulations utilizing Newton's classical equations. Preprocessing, optimization, and minimization of complexes were done with Maestro's Protein Preparation Wizard [29]. To avoid interactions with periodic

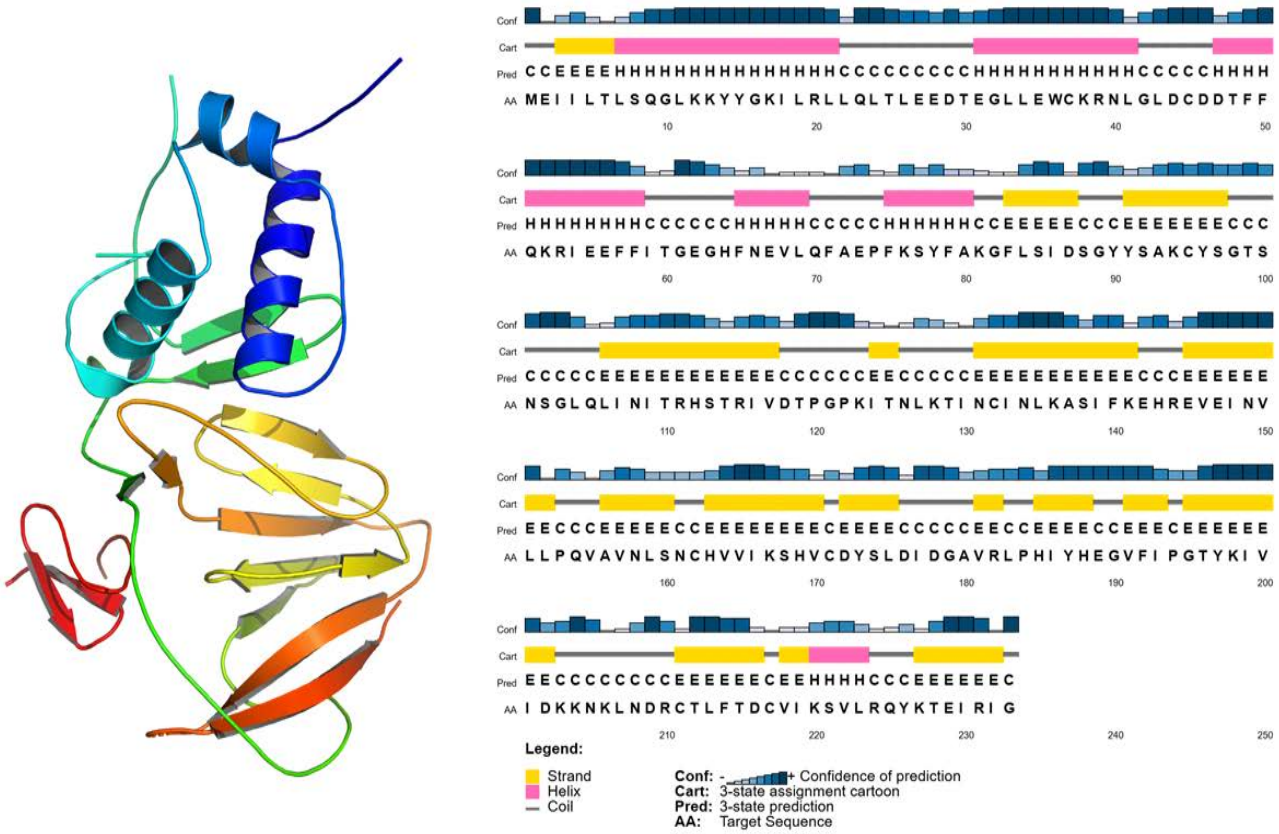

Figure 2. The left side displays the three-dimensional structure of the Crimean-Congo hemorrhagic fever virus's glycoprotein, while the right side displays the secondary structure.

pictures, the system was housed in an orthorhombic simulation box with a minimum gap of 10 Å between the protein and the box edges. Using the System Builder tool, the system was created using the OPLS_2005 force field, the TIP3P solvent model, and 0.15 M sodium chloride to simulate physiological circumstances[30]. The NPT ensemble was used with a temperature control of 300 K and a pressure of 1 atm. A thorough examination of the system dynamics throughout time was made possible by the saving of trajectories at 100 ps intervals. The R package "Bio3D" was also used to assess the dynamic cross-correlation matrix (DCCM) and principal component analysis (PCA)[31] (Figure 1).

RESULTS

Target protein retrieval and Physicochemical properties analysis: The structural protein of Crimean–Congo hemorrhagic fever retrieved from PDB having resolution 1.80 Å and 233 amino acids. The molecular weight of 8VVL protein is 26632.83 and the Instability index shows that this protein is stable. GRAVY score indicated that the protein has hydrophilic nature. Theoretical PI value is 8.06 and the estimated half-life in mammalian reticulocytes is 30 hours (Table 1). PSIPRED analysis of Crimean–Congo hemorrhagic fever protein was shown in Figure 2. The confidence score indicated the certainty and uncertainty in several regions. The score ranges from 0 to 9 which indicates greater confidence score in the prediction[32]. The alpha helices, strands and coils were represented in pink, yellow and grey. This chart shows that there is a low proportion of alpha helices as compared to beta sheets and coils (Figure 2).

Table 1. Physiochemical properties of target protein of Crimean-Congo hemorrhagic fever virus

Sr. no	Properties	Protein
1	no. of amino acids	233
2	molecular weight	26632.83
3	Theoretical pI	8.06
4	instability index (II)	33.70 (stable)
5	Aliphatic index	102.02
6	Estimated half-life	30 hours (mammalian reticulocytes)
7	Estimated half-life	>20 hours (yeast, in vivo)
8	Estimated half-life	>10 hours (Escherichia coli, in vivo)
9	Grand average of hydropathicity (GRAVY)	-0.113
10	extinction coefficient (M^{-1} cm^{-1}, at 280 nm measured in water)	20900 (Abs 0.1% (=1 g/l) 0.785)

Toxicity and Allergenicity and heatmap prediction of Cyclotides: Allergenicity and toxicity prediction of selected cyclotides were predicted through the AllerTOP and ToxinPred servers. There are some cyclotides which are Allergen while all are non-toxin and the SVM score also given in the Table 2. The top cyclotide's 3D structure on the base of docking score and further Kalata B7 features are displayed in Figure 3.

Table 2. The toxicity and allergenicity of the cyclotides

Cyclotides	Allergenicity	Toxicity	SVM score
Kalata B1	Non-Allergen	Non-Toxin	-1.42
Kalata B2	Non-Allergen	Non-Toxin	-1.41
Kalata B3	Non-Allergen	Non-Toxin	-1.31
Kalata B4	Non-Allergen	Non-Toxin	-1.45
Kalata B5	Allergen	Non-Toxin	-1
Kalata B6	Non-Allergen	Non-Toxin	-1.24
Kalata B7	Non-Allergen	Non-Toxin	-1.45
Kalata B8	Non-Allergen	Non-Toxin	-1
Kalata B9	Non-Allergen	Non-Toxin	-1.26
Kalata B10	Non-Allergen	Non-Toxin	-1.29
Kalata B11	Non-Allergen	Non-Toxin	-1.38
Kalata B12	Non-Allergen	Non-Toxin	-0.82
Kalata B13	Allergen	Non-Toxin	-1.19
Kalata B14	Allergen	Non-Toxin	-1
Kalata B15	Non-Allergen	Non-Toxin	-1.23
Kalata B16	Allergen	Non-Toxin	-1
Kalata B17	Allergen	Non-Toxin	-1
Kalata B18	Allergen	Non-Toxin	-0.89
Kalata S	Non-Allergen	Non-Toxin	-1.34

Figure 4 displays the energy values in (J per aa) Joules per amino acid from the "Energy Heatmap." The green areas are where the top selected peptide Kalata B7 shows the most stability, indicating that these circumstances are ideal for its possible application as a medication. Figure 5 shows the data in the "Charge Heatmap" as electrons per amino acid (e per aa). The heatmap's blue preponderance indicates that the Kalata B7 peptide has a comparatively constant charge under many circumstances, which is beneficial for its stability. The little red patches show that larger charge densities are present under a small number of circumstances, although they are not common.

Molecular Docking: The HDOCK server was used to forecast the complex that will form between the cyclotide Kalata B7 and the target protein 8vvl, and the data was arranged in a table 3. A simple comparison of the docking results between different cyclotides and the targeted protein was made easier by Table 3, and additional analysis was conducted using the complex with the highest docking score.

Table 3. The docking score and 3D structures of cyclotides against target protein

Cyclotides	Docking Score	3D structures
Kalata B1	-193.6	
Kalata B2	-197.4	
Kalata B3	-196.22	
Kalata B4	-188.63	
Kalata B6	-212.4	
Kalata B7	-213.76	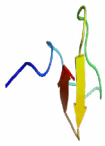
Kalata B8	-193.58	
Kalata B9	-200.88	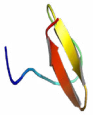
Kalata B10	-200.3	

Kalata B11	-187.19	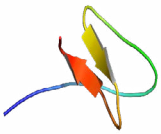
Kalata B12	-178.48	
Kalata B15	-194.03	
Kalata S	-191.13	

Interaction analysis

Kalata B7 was chosen as a potential treatment option as it had the highest docking score (-213.76) of all the complexes. Figure 6 showed the target protein's 3D docking, interaction, and binding site visualizing with Kalata B7. In figure 6A highlighting regions of contact, this map highlights the ligand's spatial arrangement with respect to the protein's active site. The red color sticks indicate the ligand, while the green protein sphere represents the amino acid residues of the targeted protein that are engaged in binding interactions.

Table 4. Physiochemical properties of top Cyclotide Kalata B7

Sr. no	Properties	Cyclotide Kalata B7
1	no. of amino acids	29
2	molecular weight	3095.60
3	Theoretical pI	7.77
4	instability index (II)	49.86
5	Aliphatic index	50.34
6	Estimated half-life	30 hours (mammalian reticulocytes)
7	Estimated half-life	>20 hours (yeast, in vivo)
8	Estimated half-life	>10 hours (Escherichia coli, in vivo)
9	Grand average of hydropathicity (GRAVY)	0.038
10	extinction coefficient (M^{-1} cm^{-1}, at 280 nm measured in water)	7365 (Abs 0.1% (=1 g/l) 2.379)

Molecular Dynamic Simulation: The RMSD of the ligand (Kalata B7 in red) and receptor (protein in blue) is shown in Figure 7. In comparison to the ligand, the receptor exhibits a high degree of flexibility with RMSD values of around 3.4 Å[33]. The ligand's structure appears to be stable based on its reduced and steady RMSD values (~2.5 Å).

In Figure 8, the RMSF is shown. The flexible portions of the receptor are represented by certain residues that exhibit substantial variations[34]

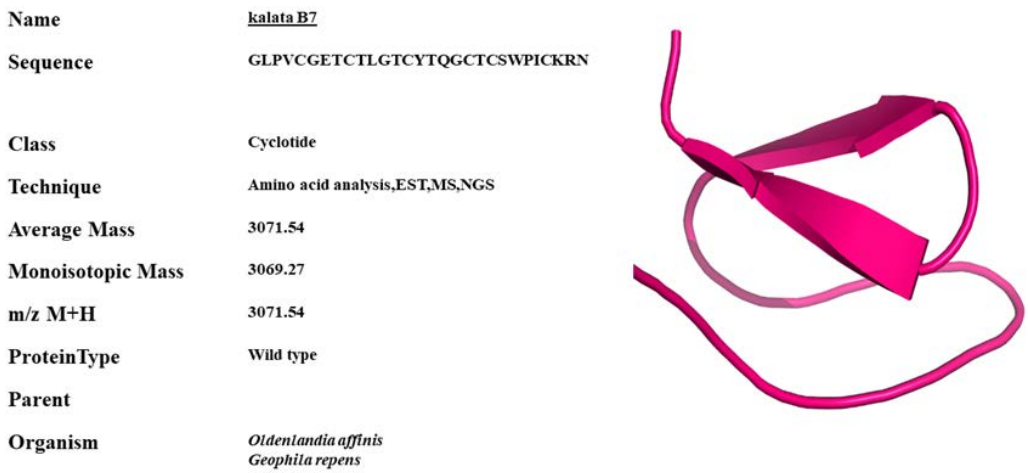

Figure 3. 3D Structure visualization and details of top Cyclotide Kalata B7

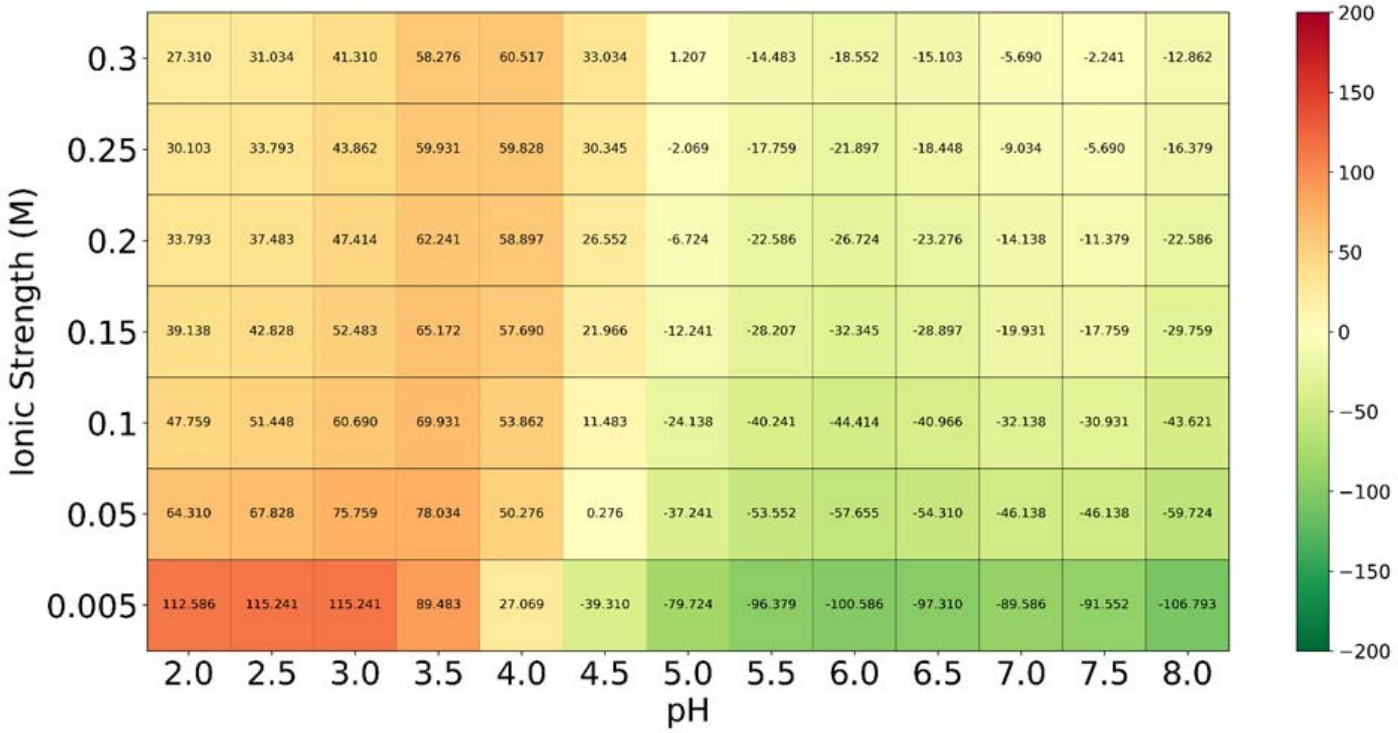

Figure 4. This heatmap shows how the energy levels of the peptide change under various scenarios. Red spots in this illustration denote lesser stability (more energy), whereas green portions show higher stability (lower energy).

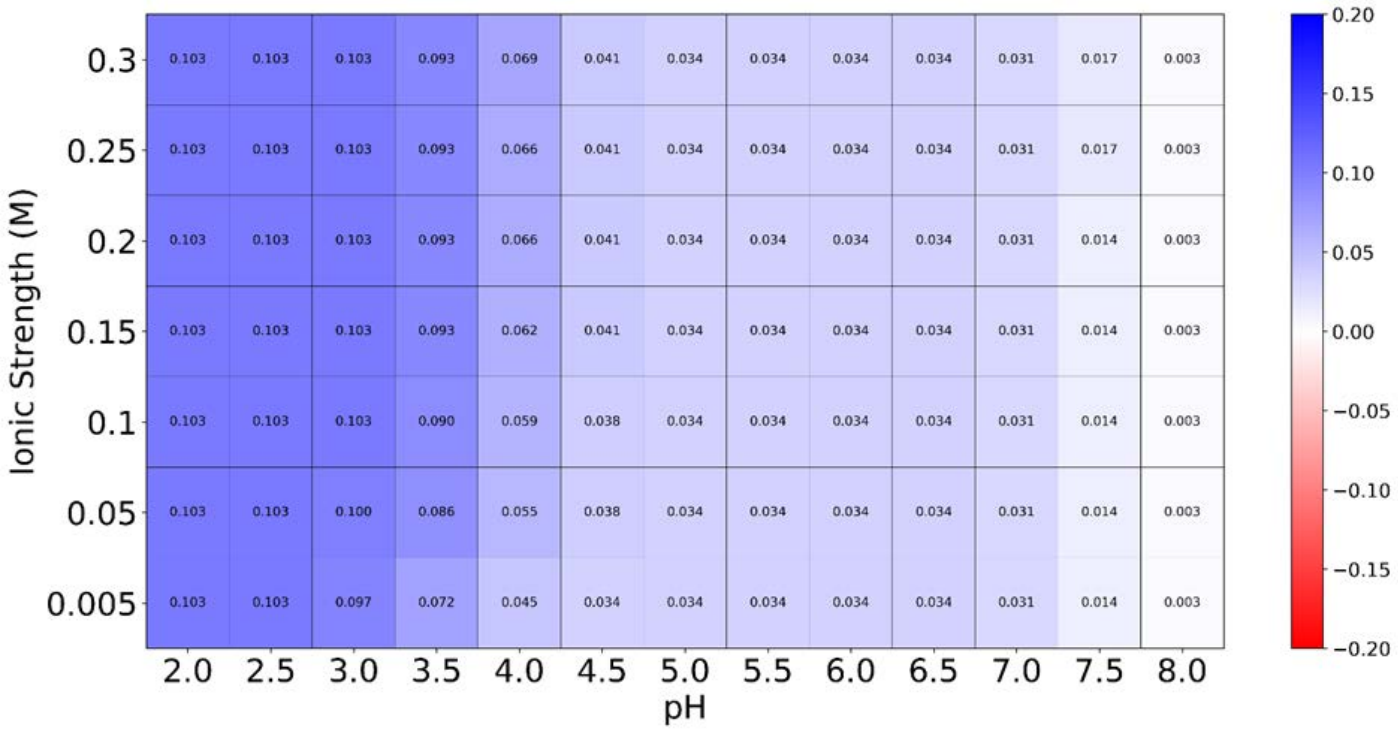

Figure 5. This heatmap offers information about how the peptide charges under different circumstances. Red indicates a high charge density, whereas blue denotes a low charge density.

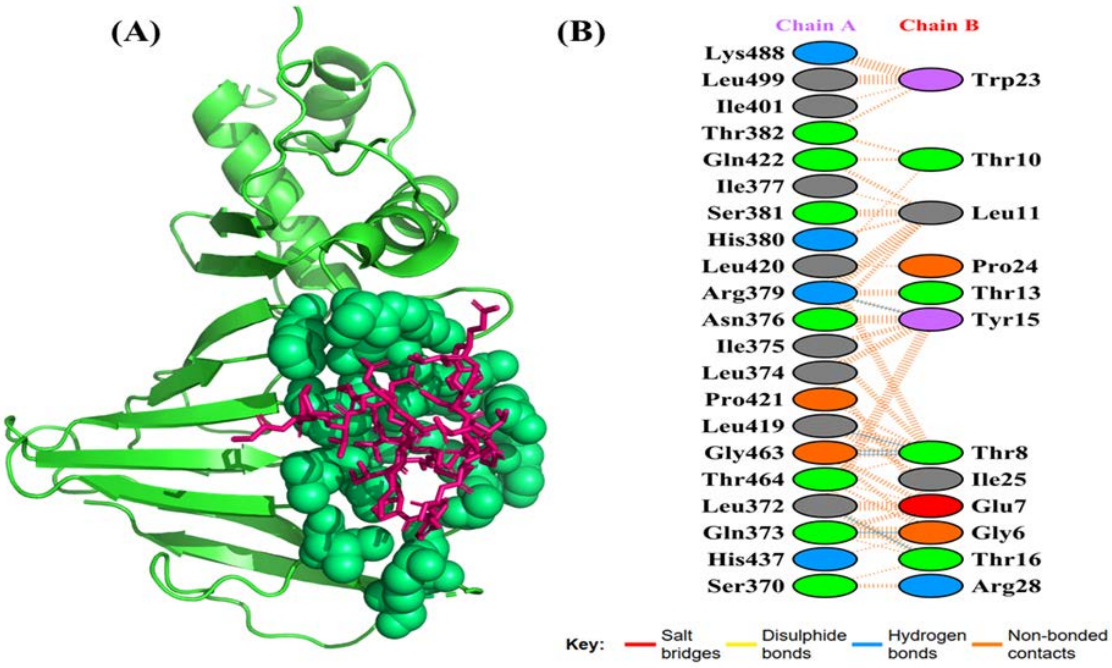

Figure 6. Target protein docking imaging in three dimensions using the cyclotide Kalata B7. (A) The protein's molecular surface is depicted in green in the image, while green spheres represent the active site. The bound ligand region inside the protein's binding pocket is shown by red sticks. (B) The docking interaction analysis PDBsum is displayed in the figure. The receptor protein is denoted by chain A, whereas the ligand (Kalata B7) is denoted by chain B.

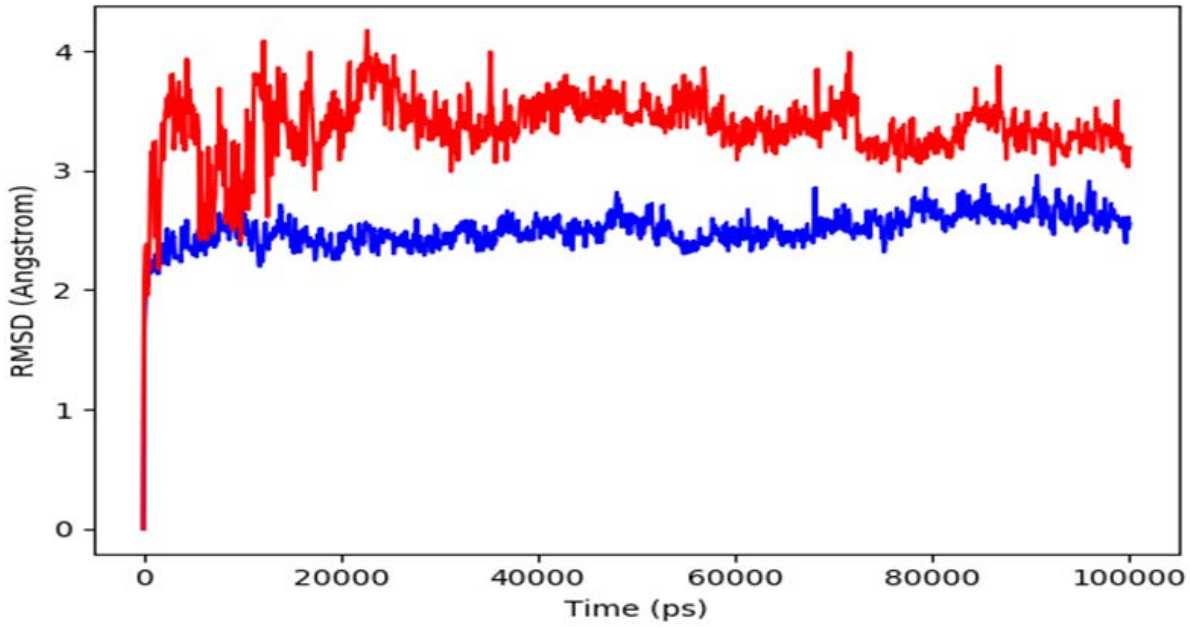

Figure 7. Kalata B7 (red) and receptor (blue) RMSD across the simulation period demonstrated ligand stability and receptor flexibility.

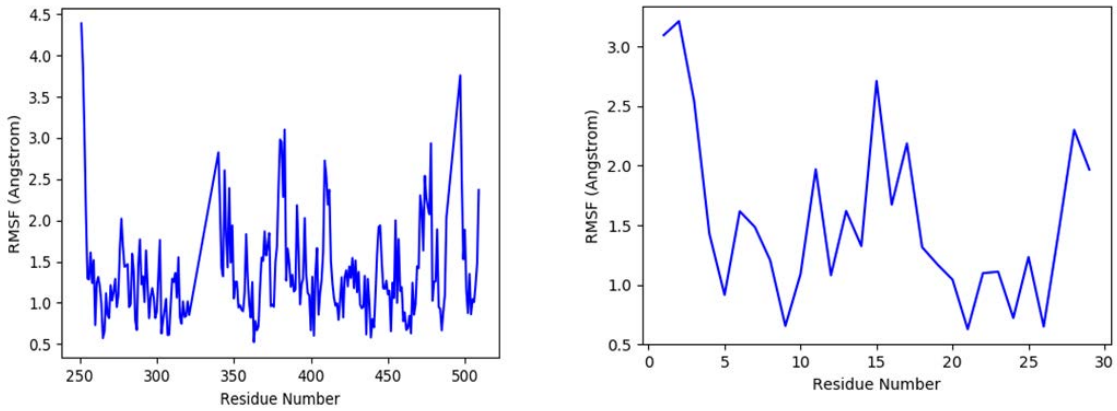

Figure 8. RMSF of Kalata B7 (B) and receptor protein (A) across the simulation period demonstrated ligand stability and receptor flexibility.

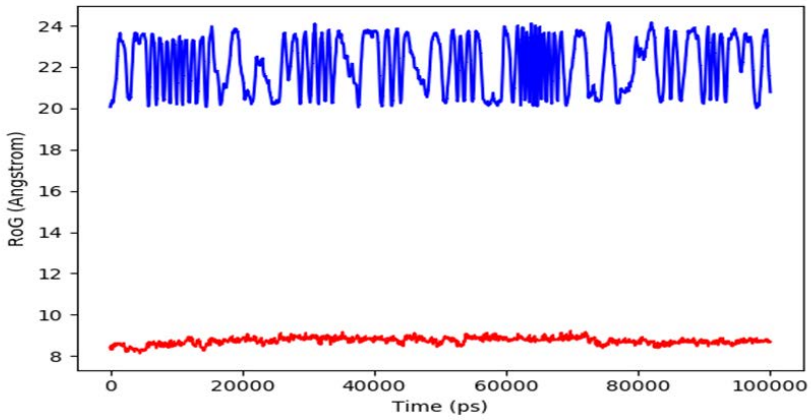

Figure 9. The extended receptor and more compact ligand are indicated by the radius of gyration of the receptor protein (blue) and Kalata B7 (red) over time.

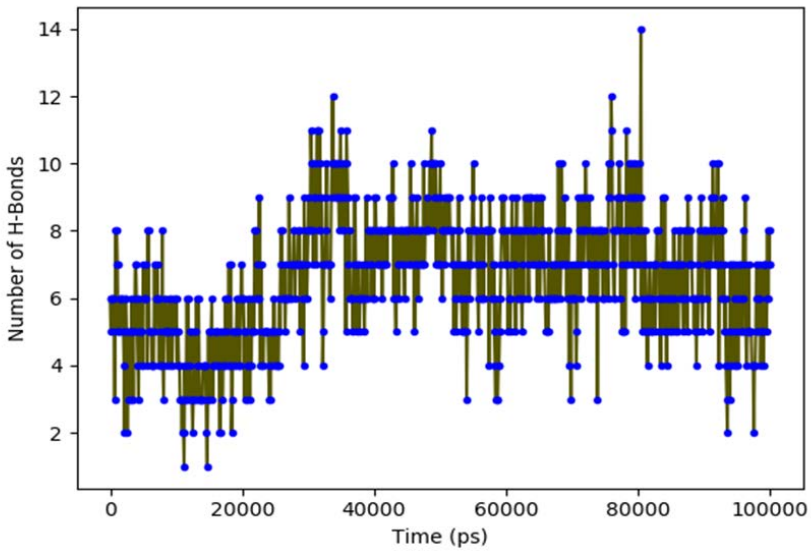

Figure 10. Protein and Kalata B7 dynamic binding interactions with respect to the quantity of hydrogen bonds throughout time.

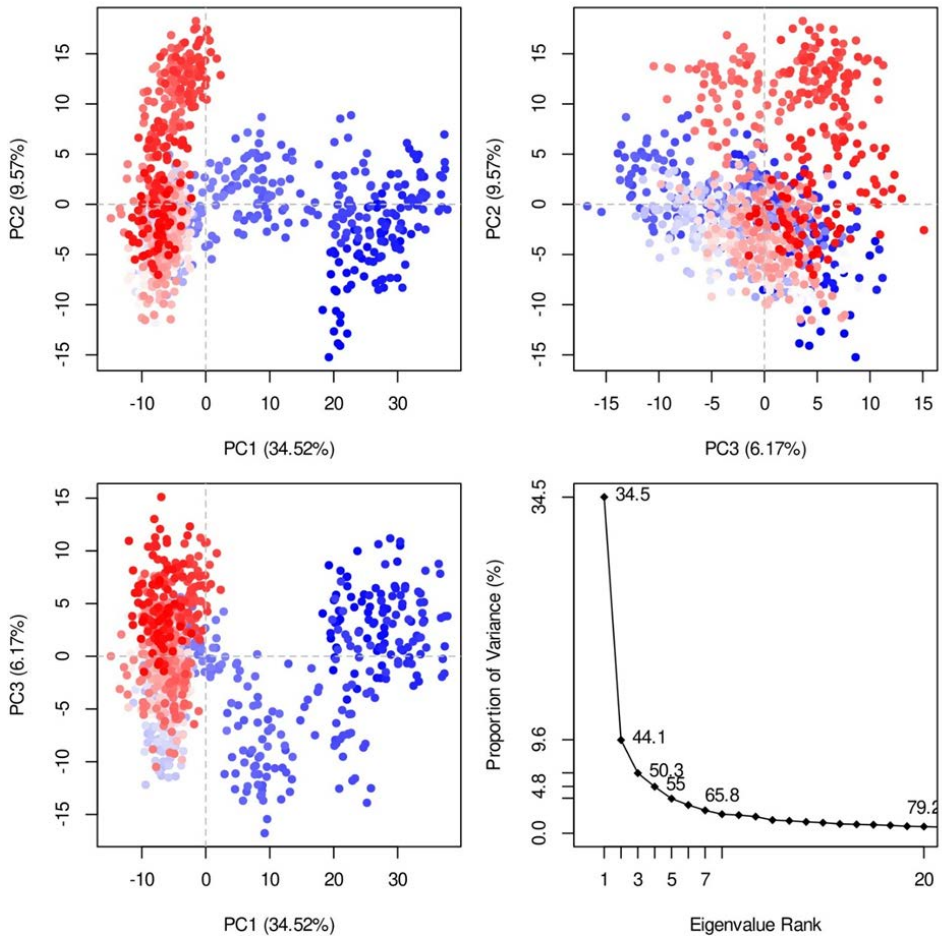

Figure 11. Depicts the PCA diagram of the complex 8vvl- Kalata B7

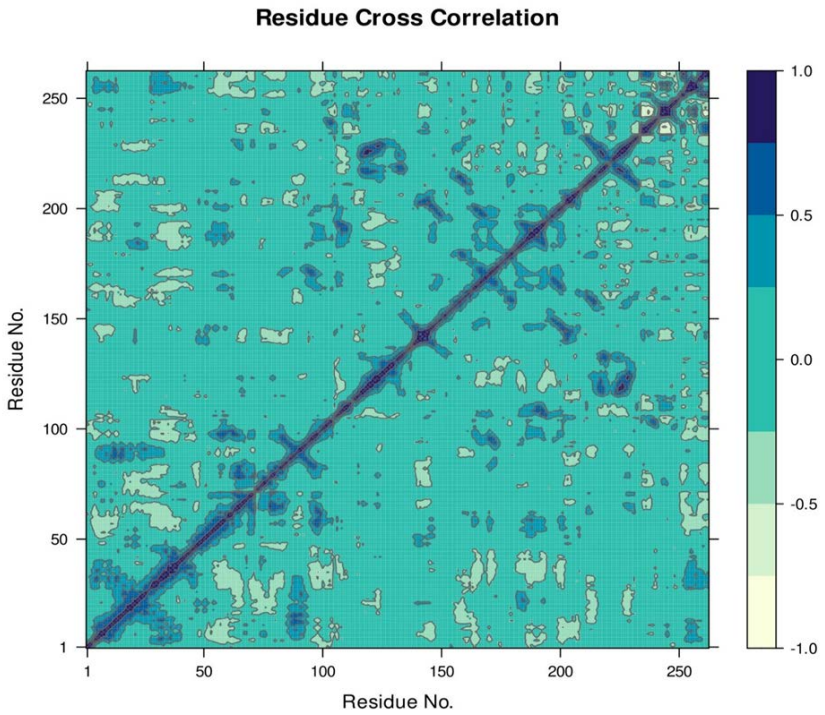

Figure 12. Depicts the DCCM diagram of the complex 8vvl- Kalata B7

(Figure 8A). The ligand's significantly reduced RMSF values indicate that it is firmly attached to the receptor (Figure 8B).

The receptor displays a large radius of gyration (~14 Å) in Figure 9, indicating a stable yet extended conformation[35]. The ligand's structure is compact and stable, as evidenced by its reduced and steady radius of gyration (~7 Å).

With a peak of roughly 13 bonds, Figure 10's hydrogen bond count demonstrates a consistently high number of interactions between the ligand and receptor, highlighting the complex's stability and robustness over the course of the simulation[36].

According to the PCA diagram, the first three panels, which depict the separation of distinct conformations, show the clustering of data points along PC1 vs. PC2 (34.52% vs. 9.57% variance explained), PC2 vs. PC3 (9.57% vs. 6.17% variance explained), and PC1 vs. PC3 (34.52% vs. 6.17% variance explained), respectively[37]. The scree plot, which shows the percentage of variance explained by each principle component and shows that the first few components capture the most important variation, is displayed in the fourth panel. 34.52% of the variation is explained by the first principal component (PC1), 9.57% by PC2, 6.17% by PC3, and increasingly smaller values by the remaining components.

Figure 12 displays the DCCM graph, which reveals the dynamic connection between the residues in an organism's protein structure. The dynamic correlation between an receptor 8vvl protein structure's residues is provided by the DCCM[38]. In this instance, negative correlations are lighter shades of blue and demonstrate that the motions are counteractive, whereas positive correlations are dark blue and reflect interacting movements.

DISCUSSION

The target protein for the Crimean-Congo hemorrhagic fever virus used in this study was acquired from the Protein Data Bank (PDB) using the ID 8VVL. PyMol was used to clean and show the protein structure. The physicochemical characteristics of the protein were predicted using the secondary structure predicted by PSIPRED and the ProtParam program on the ExPASy website. At 280 nm, the extinction coefficient is high (20900 M^{-1} cm^{-1}), indicating strong absorbance, which is characteristic of aromatic amino acids. The protein's moderate aliphatic index of 102.02 and low instability index of 33.70 contribute to its stability. The protein is hydrophilic based on its negative GRAVY score of -0.113 (Table 1). The determined theoretical isoelectric point (pI) of the protein is 8.06, indicating that it is basic and that pH can influence its solubility and characteristics. Proteins are predicted to have a net positive charge at pH values lower than 8.06, which might cause precipitate and reduced solubility.

The HDOCK program was used for docking research in order to forecast how the protein would interact with possible cyclotides. Because Kalata B7 represented the complex with the highest docking score (-213.76) out of all the complexes produced by docking calculations, it was selected as the best medication candidate (Table 3). The docking complex between the receptor's amino acids and the ligand cyclotide showed a substantial binding affinity, according to interaction analysis[39]. A protein known as Kalata B7 was extracted from the Oldenlandia affinis Geophila repens plant. Amino acid analysis, EST, MS, and NGS approaches were used to describe it[40]. It has a specific amino acid order. Since Kalata B7 is a wild-type protein, it has not undergone any genetic modification. Kalata B7, which has an SVM score of -1.45, is regarded as non-toxic, nontoxic, and does not trigger allergic responses. AlgPred and ToxinPred, respectively, were used to forecast this attribute of toxicity and allergenicity[41]. It has 415 atoms and 29 amino acids, with a molecular weight of 3095.60, based on the physiochemical characteristics predicted by ProtParam. There are not many charged amino acids in this cyclotide, and the protein's extinction coefficients vary according on the cysteine residues' oxidation state (Table 4). Kalata B7's Aliphatic Index of 50.34 indicates that it is somewhat stable. The protein's theoretical pI is 7.77, indicating that it is somewhat basic, while its GRAVY score of 0.038 indicates that it is moderately hydrophobic.

Using Desmond from Schrödinger LLC, MD simulations were run for 100,000 picoseconds. Using the R package "Bio3D," PCA and DCCM were also assessed. The results show that some protein areas exhibit structural flexibility, which may be essential for the protein's biological function or ability to interact with ligands (cyclotides)[42]. The low RMSD and RMSF values as well as the strong protein binding relationship provide additional evidence for Kalata B7's structural stability. The compact structure of Kalata B7 guarantees its stable engagement with the receptor, whereas the radius of gyration value shows that the protein maintains an extended shape. The binding affinities vary at different times during the simulation, which may indicate that the ligand-receptor relationship is flexible. The fluctuations in the hydrogen bonds indicate that the affinity of the binding contact is not in an equilibrium condition. regarded favorably, because it is known that the ligand and target have a modest level of binding.

In the present work, the protein and cyclotides are involved; the protein structure is observed in Chimera, the interaction between the two is examined in PyMol, and toxicity and allergenicity are predicted using ToxinPred and AlgPred, respectively, using HDOCK for docking. Kalata B7 has the greatest docking score (-213.76) and molecular dynamics, which provide details on binding stability and conformational changes over time, validate the simulations' structural stability and safety. The use of Insilco analysis in the current work can be seen as thorough and forward-looking. Given the methods employed in the current study, the implications suggest possible sources of novel drugs, including plant-derived cyclotides against the Crimean-Congo hemorrhagic fever virus, which are essential for the development of new antibiotics to address this new health concern and may provide a more effective method of finding new drugs.

CONCLUSIONS

The best medication candidate against Crimean-Congo hemorrhagic fever virus was Kalata B7, which inhibited the envelope glycoprotein with the highest docking score (-213.76). It exhibits no toxicity or allergenicity. Additionally, it demonstrated positive findings from dynamic simulations and molecular docking, and it may be a great medication for clinical use. Additional in vitro and in vivo research should be conducted in the future to verify Kalata B7's efficacy and toxicity.

Authorship Contribution: The study was conceptualized, designed, and conducted by Mansoor Alsahag. Material preparation, data collection, analysis, and manuscript writing were solely performed by the author. The author has read and approved the final manuscript.

Potential Conflicts of Interest: None

Competing Interest: None

Acceptance Date: 12 May 2025

REFERENCE

1. Whitehouse CA. Crimean–Congo hemorrhagic fever. Antiviral Res. 2004;64(3):145-60.
2. Watts DM, Al-Nakib W, Botros B, Saluzzo JF, Takeda N, et al. Crimean-Congo hemorrhagic fever. Infect Dis Rev. 2019;177-222.
3. Ergönül Ö. Crimean-Congo haemorrhagic fever. Lancet Infect Dis. 2006;6(4):203-14.
4. Ilboudo AK, Diallo A, Sow O, et al. Spatial analysis and risk mapping of Crimean-Congo hemorrhagic fever (CCHF) in Sub-Saharan Africa. Epidemiol Glob Health. 2025;15(1):2292.
5. Hoogstraal H. The epidemiology of tick-borne Crimean-Congo hemorrhagic fever in Asia, Europe, and Africa. J Med Entomol. 1979;15(4):307-17.
6. Osborne JC. Interactions of Bunyamwera Virus Nucleocapsid Protein and Encapsidation of Viral RNA. [Thesis]. University of Glasgow; 2001.
7. Maotoana MG. Characterization of T cell responses to the non-structural proteins of the M segment in survivors of Crimean-Congo haemorrhagic fever. [Thesis]. University of the Free State; 2019.
8. Andersson I. Crimean-Congo Hemorrhagic Fever Virus: interferon-induced antiviral mechanisms and immune evasion strategies. [Thesis]. Karolinska Institutet; 2008.
9. Frank MG, Weaver G, Raabe V. Crimean-Congo Hemorrhagic Fever Virus for Clinicians—Epidemiology, Clinical Manifestations, and Prevention. Emerg Infect Dis. 2024;30(5):854-63.
10. Karanam SK, Awasthi R, Kumar A, et al. Crimean-Congo hemorrhagic fever: Pathogenesis, transmission, and public health challenges. J Infect Public Health. 2025;14(1):XX-XX.
11. Tabassum S, Khan M, Alam S, et al. Crimean-Congo hemorrhagic fever outbreak in Pakistan, 2022: A warning bell amidst unprecedented floods and COVID-19 pandemic. Health Sci Rep. 2023;6(1):e1055.
12. Mertens M, Schmidt K, Ozkul A, et al. The impact of Crimean-Congo hemorrhagic fever virus on public health. Infect Dis Rev. 2013;98(2):248-60.
13. Leblebicioglu H, Sunbul M, Ozaras R, et al. Consensus report: Preventive measures for Crimean-Congo Hemorrhagic Fever during Eid-al-Adha festival. Int J Infect Dis. 2015;38:9-15.
14. Mardani M, Keshtkar JM. Crimean-Congo hemorrhagic fever. Bahrain Med Bull. 2007;XX(X):XX-XX.
15. de Veer SJ, Weidmann J, Craik DJ. Cyclotides as tools in chemical biology. Acc Chem Res. 2017;50(7):1557-65.
16. Ojeda PG, Cardoso MH, Franco OL. Pharmaceutical applications of cyclotides. Drug Discov Today. 2019;24(11):2152-61.
17. Yuan S, Chan HCS, Hu Z. Using PyMOL as a platform for computational drug design. Wiley Interdiscip Rev Comput Mol Sci. 2017;7(2):e1298.
18. Bank PD. Protein Data Bank. Nature New Biol. 1971;233(223):10-1038.
19. Gasteiger E, Hoogland C, Gattiker A, et al. ExPASy: The proteomics server for in-depth protein knowledge and analysis. Nucleic Acids Res. 2003;31(13):3784-8.
20. McGuffin LJ, Bryson K, Jones DT. The PSIPRED protein structure prediction server. Bioinformatics. 2000;16(4):404-5.
21. Mulvenna JP, Wang C, Craik DJ. CyBase: A database of cyclic protein sequence and structure. Nucleic Acids Res. 2006;34(Database issue):D192-4.
22. Du Z, Su H, Wang W, et al. The trRosetta server for fast and accurate protein structure prediction. Nat Protoc. 2021;16(12):5634-51.
23. Rathore AS, Sharma V, Gupta R, et al. ToxinPred 3.0: An improved method for predicting the toxicity of peptides. Comput Biol Med. 2024;179:108926.
24. Dimitrov I, Flower DR, Doytchinova I. AllerTOP—a server for in silico prediction of allergens. BMC Bioinformatics. 2013;14(6):S4.
25. Hebditch M, Warwicker J. Web-based display of protein surface and pH-dependent properties for assessing the developability of biotherapeutics. Sci Rep. 2019;9(1):1969.
26. Yan Y, Tao H, He J, et al. The HDOCK server for integrated protein–protein docking. Nat Protoc. 2020;15(5):1829-52.
27. Laskowski RA, Thornton JM. PDBsum extras: SARS-CoV-2 and AlphaFold models. Protein Sci. 2022;31(1):283-9.
28. Ullah S, Fatima S, Iqbal M, et al. A computational approach to fighting type 1 diabetes by targeting 2C Coxsackie B virus protein with flavonoids. PLoS One. 2023;18(8):e0290576.
29. Oluwafemi KA, Singh A, Choudhury A, et al. Investigating the effect of 1,2-Dibenzoylhydrazine on Staphylococcus aureus using integrated computational approaches. In Silico Pharmacol. 2024;12(2):102.
30. Shivakumar D, Williams J, Wu Y, et al. Prediction of absolute solvation free energies using molecular dynamics free energy perturbation and the OPLS force field. J Chem Theory Comput. 2010;6(5):1509-19.
31. Grant BJ, Skjærven L, Yao XQ. The Bio3D packages for structural bioinformatics. Protein Sci. 2021;30(1):20-30.
32. Buchan DWA, Ward SM, Lobley AE, et al. Scalable web services for the PSIPRED Protein Analysis Workbench. Nucleic Acids Res. 2013;41(W1):W349-57.
33. Carugo O. How root-mean-square distance (RMSD) values depend on the resolution of protein structures that are compared. J Appl Crystallogr. 2003;36(1):125-8.
34. da Fonseca AM, et al. Screening of potential inhibitors targeting the main protease structure of SARS-CoV-2 via molecular docking. Mol Biotechnol. 2024;66(8):1919-33.
35. Lobanov MY, Bogatyreva NS, Galzitskaya OV. Radius of gyration as an indicator of protein structure compactness. Mol Biol 2008; 42:623-8.
36. Voloshin VP, Naberukhin YI. Hydrogen bond lifetime distributions in computer-simulated water. J Struct Chem 2009; 50:78-89.
37. Palma J, Pierdominici-Sottile G. On the uses of PCA to characterise molecular dynamics simulations of biological macromolecules: basics and tips for an effective use. ChemPhysChem 2023; 24(2):e202200491.
38. Gyawali K, Acharya A, Pandit P, et al. Identification of catechin as main protease inhibitor of SARS-CoV-2 Omicron variant using molecular docking, molecular dynamics, PCA, DCCM, MM/GBSA and ADMET profiling. Nat Prod Res 2024; 1-8.
39. Li H, Gao Y, Liu G, et al. HDOCK update for modeling protein-RNA/DNA complex structures. Protein Sci 2022; 31(11):e4441.
40. Shenkarev ZO, Nadezhdin KD, Sobol AG, et al. Divalent cation coordination and mode of membrane interaction in cyclotides: NMR spatial structure of ternary complex Kalata B7/Mn2+/DPC micelle. J Inorg Biochem 2008; 102(5-6):1246-56.
41. Tu M, Cheng Y, Xie C, et al. Bioactive hydrolysates from casein: generation, identification, and in silico toxicity and allergenicity prediction of peptides. J Sci Food Agric 2018; 98(9):3416-26.
42. Rasheed MA, Iram A, Saeed M, et al. Identification of lead compounds against Scm (fms10) in Enterococcus faecium using computer-aided drug designing. Life 2021; 11(2):77.